Ad Hoc Networks 11 (2013) 1331–1344

Contents lists available at ScienceDirect

Ad Hoc Networks

journal homepage: www.elsevier.com/locate/adhoc

Three-dimensional greedy routing in large-scale random wireless sensor networks

Yu Wang [a,*], Chih-Wei Yi [b], Minsu Huang [a], Fan Li [c]

[a] Department of Computer Science, University of North Carolina at Charlotte, Charlotte, NC 28223, United States
[b] Department of Computer Science, National Chiao Tung University, Hsinchu City 30010, Taiwan, ROC
[c] School of Computer Science, Beijing Institute of Technology, Beijing 100081, China

ARTICLE INFO

Article history:
Available online 12 October 2010

Keywords:
Greedy routing
Localized routing
Delivery guarantee
Energy-efficiency
3D wireless sensor networks

ABSTRACT

In this paper, we investigate how to design greedy routing to achieve sustainable and scalable in a large-scale three-dimensional (3D) sensor network. Several 3D position-based routing protocols were proposed to seek either delivery guarantee or energy-efficiency in 3D wireless networks. However, recent results [1,2] showed that there is no deterministic localized routing algorithm that guarantees either delivery of packets or energy-efficiency of its routes in 3D networks. In this paper, we focus on design of 3D greedy routing protocols which can guarantee delivery of packets and/or energy-efficiency of their paths with high probability in a *randomly* deployed 3D sensor network. In particular, we first study the asymptotic critical transmission radius for 3D greedy routing to ensure the packet delivery in large-scale random 3D sensor networks, then propose a refined 3D greedy routing protocol to achieve energy-efficiency of its paths with high probability. We also conduct extensive simulations to confirm our theoretical results.

1. Introduction

Most existing wireless sensor systems and protocols are based on two-dimensional (2D) design, where all wireless sensor nodes are distributed in a two-dimensional plane. This assumption is somewhat justified for applications where sensor nodes are deployed on earth surface and where the height of the network is smaller than transmission radius of a node. However, 2D assumption may no longer be valid if a wireless sensor network is deployed in space, atmosphere, or ocean, where nodes of a network are distributed over a 3D space and the difference in the third dimension is too large to be ignored. In fact, recent interest in under-water sensor networks [3] or space sensor networks [4] hints at the strong need to design 3D wireless networks. However, the design of networking protocols for 3D wireless networks is surprising more difficult than that for 3D networks. In this paper, we focus on one particular problem in 3D networks: 3D localized position-based routing.

Localized position-based routing makes the forwarding decision based solely on the position information of the destination and local neighbors. It does not need the dissemination of route discovery information and the maintenance of routing tables. Thus, it enjoys the advantages of lower overhead and higher scalability than other traditional routing protocols. This makes localized routing protocols much suitable for large-scale sensor networks. The most common and efficient localized routing is *greedy routing*, in which a packet is greedily forwarded to the closest node to the destination in order to minimize the average hop-count. Greedy routing can be easily extended to 3D case. Actually, several under-water routing protocols [5,6] are just variations of 3D greedy routing. Fig. 1 illustrates the basic idea of 3D greedy routing. Let t be the destination node. As shown in Fig. 1a, current node u finds the next relay node v who is the closest to t among all neighbors of u. But, it is easy to construct an example (see

* Corresponding author. Tel.: +1 7046878443; fax: +1 7046873516.
E-mail addresses: yu.wang@uncc.edu (Y. Wang), yi@cs.nctu.edu.tw (C.-W. Yi), mhuang4@uncc.edu (M. Huang), fli@bit.edu (F. Li).

1570-8705/$ - see front matter © 2010 Elsevier B.V. All rights reserved.
doi:10.1016/j.adhoc.2010.10.003

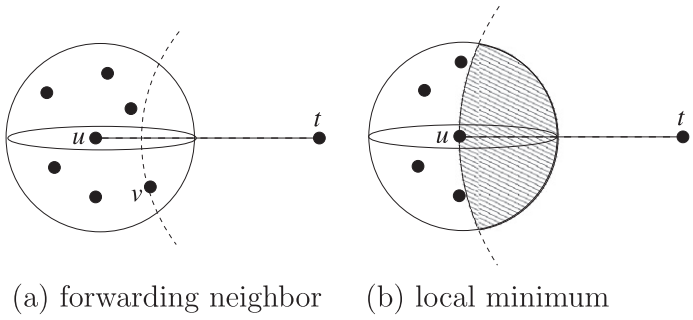

Fig. 1. Illustration of greedy routing in 3D networks.

Fig. 1b) to show that greedy routing will not succeed to reach the destination but fall into a local minimum (at a node without any "better" or "closer" neighbors). This is true for both 2D and 3D networks.

However, to guarantee *packet delivery* of 3D greedy routing is not straightforward and very challenging. Face routing can be used on planar topology to recovery from the local minimum of greedy routing and guarantee the delivery in 2D networks, as did in many 2D localized routing protocols [7–9]. However, there is no planar topology concept any more in 3D networks and simple projection from 3D to 2D may break the network connectivity. In fact, Durocher et al. [1] recently proved that there is *no* deterministic localized routing algorithm for 3D networks that guarantees the delivery of packets. On the other hand, even a localized routing method can find the route to deliver the packet, it may not guarantee the energy-efficiency of the path, *i.e.*, the total power consumed compared with the optimal could be very large in the worst case. Several energy-aware localized 2D routing protocols [10–12] already took the energy concern into consideration, but none of them can theoretically guarantee the energy-efficiency of their routes. This is true for all existing 3D localized routing methods too. Recently, Flury and Wattenhofer [2] showed an example 3D network where the path found by *any* deterministic localized routing protocol to connect two nodes s and t has energy-consumption asymptotically at least $\Theta(d^3)$ in the worst case. Here d is the optimal energy-consumption to connect s and t.

Therefore, in this paper, we are interested in (1) how to achieve delivery guarantee of 3D greedy routing in large-scale random networks; and (2) how to achieve energy-efficiency of paths in large-scale 3D networks so that the networks can be sustainable. In particular, we make the following contributions on 3D greedy routing:

- We prove that 3D greedy routing can guarantee the delivery of packets between any source–destination pairs if the underlying topology is Delaunay translation.
- We study on the *critical transmission radius* (CTR) of 3D greedy routing that guarantees the delivery of packets between any source–destination pairs. We prove that for a 3D random network, formed by nodes that are generated by a Poisson point process of density n over a convex compact region of unit-volume, the CTR for 3D greedy routing is *asymptotic almost surely* (a.a.s). at most $\sqrt[3]{\frac{3\beta \ln n}{4\pi n}}$ for any $\beta > \beta_0$ and at least $\sqrt[3]{\frac{3\beta \ln n}{4\pi n}}$ for any $\beta < \beta_0$. Here, $\beta_0 = 3.2$.
- We extend our previous 2D energy-aware routing method [13] to an *energy-efficient restricted 3D greedy routing*, which is a simple variation of 3D greedy routing. The proposed routing method can guarantee energy-efficiency of its path with high probability if it finds one in 3D networks. We also study its CTR in random 3D networks and show it is in the same formation of that of 3D greedy routing, except for $\beta_0 = \frac{2}{1-\cos\alpha}$ where α is an parameter used by the proposed method.
- We conduct extensive simulations on 3D random networks to study the distributions of CTRs of both 3D greedy routing and restricted 3D greedy routing and evaluate their routing performances.

The rest of the paper is organized as follows. In Section 2, we first review related work on 3D position-based routing and critical transmission radius of greedy routing. Then we present our network model and several preliminaries in Section 3. In Section 4, we study how to achieve delivery guarantee of 3D greedy routing by deriving the *asymptotic almost sure* bounds on the critical transmission radius of 3D greedy routing. In Section 5, we further extend the 3D greedy routing to an energy-efficient localized routing and derive its CTR bounds. We present simulation results in Section 6 and summarize this paper in Section 7.

2. Related work

Due to its wide-range potential applications, 3D wireless sensor network has recently emerged as a premier research topic. Most current research in 3D sensor networks primarily focuses on coverage [14–17], connectivity [15,18–20], and routing issues [5,6,21–24]. Since we focus on design of 3D position-based localized routing in this paper, we will first review the status on 3D position-based localized routing.

2.1. 3D localized routing: delivery guarantee and energy-efficiency

As the most widely used position-based routing, greedy routing has been used by Pompili and Melodia and Xie et al. [5,6] for 3D under-water sensor networks. However,

all of these greedy-based routings cannot guarantee the delivery, since they may fail at the local minimum. In 2D networks [7–9], delivery guarantee can be achieved by applying face routing as a backup method to get out of the local minimum after simple greedy heuristic fails. The idea of face routing is to walk along the faces which are intersected by the line segment st between the source s and the destination t. To guarantee the packet delivery, face routing requires the underlying 2D routing topology to be a planar graph (*i.e.*, no link/edge intersection). However, 3D networks cannot be planarized any more. Fevens et al. [21,22] proposed several 3D position-based routing protocols and tried to find a way to still use face routing to get out of the local minimum. Their basic idea is projecting the 3D network to a 2D plane (as shown in Fig. 2a), then applying the face routing in the plane. However, as shown in Fig. 2b [21], a planar graph cannot be extracted from the projected graph. It is clear that removing either $v'_3v'_4$ or $v'_1v'_2$ will break the connectivity. Furthermore, Durocher et al. [1] have recently proven that *there is no deterministic localized routing algorithm for 3D networks that guarantees the delivery of packets*. Flury and Wattenhofer [2] then proposed a randomized 3D routing which adopts a randomized recovery technique when 3D greedy fails.

Beside the delivery guarantee of packets, the energy-efficiency of paths is also very important for large-scale sensor networks. Given a routing method $\mathcal{A}$, let $\mathbf{P}_{\mathcal{A}}(s,t)$ be the path found by $\mathcal{A}$ to connect the source node s and the destination node t. A routing method $\mathcal{A}$ is called *energy-efficient* if for every pair of nodes s and t, the energy-consumption of path $\mathbf{P}_{\mathcal{A}}(s,t)$ is within a constant factor of the least energy-consumption path connecting s and t in the network. Even a 3D localized routing method can find the route to deliver the packet, it may not guarantee the energy-efficiency of the path, *i.e.*, the total power consumed compared with the optimal could be very large in the worst case. Several energy-aware localized 2D routing protocols [10–12] already took the energy concern into consideration, but none of them can theoretically guarantee the energy-efficiency of their routes. This is true for all existing 3D localized routing methods too. For path energy-efficiency, recently, Flury and Wattenhofer [2] proved that *no deterministic localized routing method is energy-efficient in 3D networks*. They proved the claim by constructing an example of a 3D network (Fig. 1 of [2]) where the path found by *any* localized routing protocol to connect two nodes s and t has energy-consumption (or hop-count or distance) asymptotically at least $\Theta(d^3)$ in the worst case, where d is the optimum cost. Therefore, we are also interested in refining 3D greedy routing into a 3D energy-
efficient routing. In particular, we extend our previous 2D energy-aware routing method [13] to an *energy-efficient restricted 3D greedy routing*.

2.2. Critical transmission radius for greedy routing

One way to guarantee the packet delivery for greedy routing in 2D/3D networks is letting all nodes have sufficiently large transmission radii to avoid the existence of local minimum. It is clear that this can be achieved when the transmission radius is infinite. Assume that V is the set of all wireless nodes in the network and each wireless node has a transmission radius r. Let $B(x,r)$ denote the open disk of radius r centered at x. Let

$$\rho(V) = \max_{\substack{(u,v)\in V^2 \\ u\neq v}} \min_{w\in B(v,\|u-v\|)} \|w-u\|. \tag{1}$$

In the equation, (u,v) is a source–destination pair. Since $w \in B(v,\|u-v\|)$, we have $\|w-v\| < \|u-v\|$. It means w is closer to v than u. If the transmission radius is not less than $\|w-u\|$,w might be the one to relay packets from u to v. Therefore, for each (u,v), the minimum of $\|w-u\|$ over all nodes on $B(v,\|u-v\|)$ is the transmission radius that ensures there is at least one node that can relay packets from u to v, and the maximum of the minimum over all (u,v)pairs guarantees the existence of relay nodes between any source–destination pair. Clearly, if the transmission radius is at least $\rho(V)$, packets can be delivered between any source–destination pairs. On the other hand, if the transmission radius is less than $\rho(V)$, there must exist some source–destination pair, *e.g.*, the (u,v)that yields the value $\rho(V)$, such that packets cannot be delivered. Therefore, $\rho(V)$ is called the *critical transmission radius* (CTR) for greedy routing that guarantees the delivery of packets between any source–destination pair of nodes among V.

Previously, several studies (*e.g.* [25–28]) focused on the critical transmission radius for certain network proper-

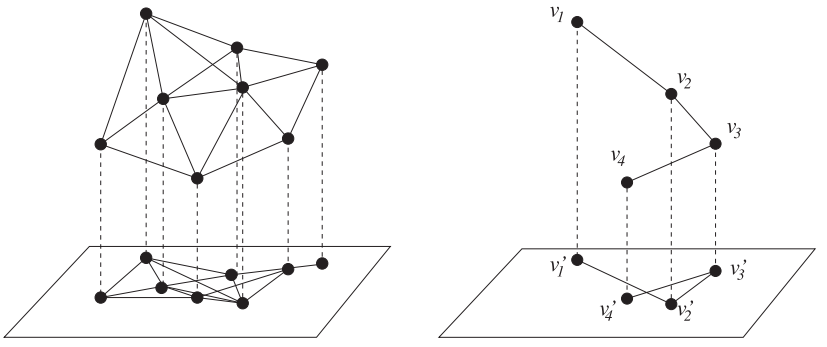

(a) 3D-2D projection (b) projection causes intersections

Fig. 2. Simple projection from 3D to 2D does not work!

ties such as connectivity, k-connectivity, and coverage. Surprisingly, there is not much study for the critical transmission radius for certain routing methods, except for the recent results [29,30] for 2D greedy routing. Traditionally it is assumed that the network nodes are represented by a Poisson point process of density n, denoted as $\mathcal{P}_n$, over a unit area disk or square. Wan et al. [29] proved that for any constant $\varepsilon > 0$, it is *a.a.s.* that $(1-\varepsilon)\sqrt{\frac{\beta_0 \ln n}{\pi n}} \leqslant \rho(\mathcal{P}_n) \leqslant (1+\varepsilon)\sqrt{\frac{\beta_0 \ln\ n}{\pi n}}$, where $\beta_0 = 1/\left(\frac{2}{3} - \frac{\sqrt{3}}{2\pi}\right)$. The same authors further improved asymptotic bounds on $\rho(\mathcal{P}_n)$ in [30]. Specifically, they proved that for any constant c, the asymptotic probability of $\rho(\mathcal{P}_n) \leqslant \sqrt{\frac{\beta_0 \ln n + c}{\pi n}}$ is at least $1 - \left(\frac{1}{1/\beta_2 - 1/3} - \frac{\beta_0}{2}\right)e^{-c}$ and at most $e^{-\frac{\beta_0}{2}e^{-c}}$. In this paper, we will apply similar techniques used by Wan et al. [29] to derive the CTR for 3D greedy routing and the proposed restricted 3D greedy routing.

3. Preliminaries

In this section, we present our models and several useful results which are used by our analysis on critical transmission radius of 3D greedy routing.

3.1. Assumptions and notations

We consider a set V of n wireless sensor devices (called nodes hereafter) uniformly distributed in a compact and convex 3D region $\mathbb{D}$ with unit-volume in $\mathbb{R}^3$. By proper scaling, we assume the nodes are represented by a Poisson point process $\mathcal{P}_n$ of density n over a unit-volume cube $\mathbb{D}$. Each node knows its position information and has a uniform transmission radius r (orr_n). Then the communication network is modeled by a unit disk graph $G(V,r)$, where two nodes u and v are connected if and only if their Euclidean distance is at most r. Hereafter, we use $\|u-v\|$ to denote the Euclidean distance between u and v. For a link $uv \in G(V,r)$, we use $\|uv\|$ to denote its length. We further assume that the energy needed to support the transmission of a unit amount of data over a link uv is $\mathbf{e}(\|uv\|)$, where $\mathbf{e}(x)$ is a non-decreasing function on x.

For a finite set S, we use $\#(S)$ to denote its cardinality. For a set $A \subset \mathbb{R}^3$, we use $|A|$ to denote the volume of A and use ∂A to denote the topological boundary of A. Let $B(x,r)$ denote the open sphere of radius r centered at x. For any two points $u, v \in \mathbb{R}^3$, the intersection of two spheres of radii $\|u-v\|$centered respectively at u and v, denoted by L_{uv}, is called the *biconvex* of u and v, *i.e.* $L_{uv} = B(u,\|u-v\|) \cap B(v,\|u-v\|)$, and $\|u-v\|$ is called the depth of the biconvex. An event is said to be *asymptotic almost sure* if it occurs with a probability converges to one as $n \to \infty$. To avoid trivialities, we assume n to be sufficiently large if necessary.

3.2. Geometric preliminaries

We first provide several geometric lemmas which will be used in the analysis of critical transmission radius of 3D greedy routing. Due to the space limit, we ignore their proofs (which are similar to those of lemmas in [29] for 2D case). If $\|u-v\| = 1$, a straightforward calculation yields that $|L_{uv}| = \frac{5\pi}{12}$. The volume of such a biconvex with respect to the volume of a unit-volume ball is $\frac{5\pi/12}{4\pi/3} = \frac{5}{16}$. Let $\beta_0 = \frac{16}{5} = 3.2$. Then, the volume of a biconvex with depth r is $\frac{1}{\beta_0}\left(\frac{4}{3}\pi r^3\right)$. The following lemma gives a lower bound of the volume of two intersecting biconvexes.

Lemma 1. *Assume $R > 0$ and $a_1, b_1, a_2, b_2 \in \mathbb{R}^3$. Let $z_1 = \frac{1}{2}(a_1+b_1), r_1 = \|a_1-b_1\|, z_2 = \frac{1}{2}(a_2+b_2)$, and $r_2 = \|a_2-b_2\|$. If $r_1, r_2 \in \left[\frac{1}{2}R, R\right], \|z_1-z_2\| \leqslant \sqrt{3}R, a_1, b_1 \notin L_{a_2b_2}$, and $a_2, b_2 \notin L_{a_1b_1}$, there exist a constant γ such that*

$$|L_{a_1b_1} \cup L_{a_2b_2}| - |L_{a_1b_1}| \geqslant \gamma R^2 \|z_1 - z_2\|.$$

For any convex compact set $C \subset \mathbb{R}^3$, we use C_{-r} to denote the set of points in C that are away from ∂C by at least r. The next lemma gives a lower bound of the volume of C_{-r}.

Lemma 2. *Given a convex compact set $C \subset \mathbb{R}^3$ with diameter at most d,*

$$|C_{-r}| \geqslant |C| - \pi d^2 r.$$

An ε-tessellation is a technique that divides the 3D space by vertical planes perpendicular to either x-axis or y-axis and horizontal planes perpendicular to z-axis into equal-size cubes, called cells, in which cells are with width ε. Without loss of generality, we assume the origin is a corner of cells. In a tessellation, a polycube is a collection of cells intersecting with a convex compact set. The x-span (and y-span, z-span, respectively) of a polycube is the distance measured in the number of cells in the x-direction (and y-direction, z -direction, respectively). If the span of a convex compact set is s and the width of cells is l, the span of the corresponding polycube is at most $\lceil s/l \rceil + 1$. We have the following lemma.

Lemma 3. *If a convex compact set S consists of m cubes and τ is a positive integer constant, the number of polycubes with span at most τ and intersecting with S is $\Theta(m)$.*

3.3. Probabilistic preliminaries

The following lemma from [29] gives a lower bound for the minimum of a collection of Poisson RVs.

Lemma 4 [29]. *Assume that $\lim_{n\to\infty} \frac{\lambda_n}{\ln n} = \beta$ for some $\beta > 1$. Let $Y_1, Y_2, \cdots, Y_{I_n}$ be I_n Poisson RVs with means at least λ_n. If $I_n = o(n\sqrt{\ln n})$, then for any $1 < \beta' < \beta$, $\min_{i=1}^{I_n} Y_i > \mathcal{L}(\beta')\ln n$ a.a.s.*

Here, $\mathcal{L}(x)$ is defined as a function $\mathcal{L}$ over $(0,\infty)$ by $\mathcal{L}(x) = x\phi^{-1}(1/x)$ when $x \geqslant 1$ and =0 otherwise. ϕ is the function over $(0,\infty)$ defined by $\phi(x) = 1 - x + x \ln x$ and ϕ^{-1} is the inverse of the restriction of ϕ to $(0,1]$. It can be verified that $\mathcal{L}$ is a monotonic increasing function of β.

At last, we state the Palm theory [31] on the Poisson process.

Theorem 5 [31]. *Let $n > 0$. Suppose $k \in N$, and $h(\mathcal{Y}, \mathcal{X})$ is a bounded measurable function defined on all pairs of the form $(\mathcal{Y}, \mathcal{X})$ with $\mathcal{X} \subset \mathbb{R}^3$ being a finite subset and $\mathcal{Y}$ being a subset of $\mathcal{X}$, satisfying $h(\mathcal{Y}, \mathcal{X}) = 0$ except when $\mathcal{Y}$ has k elements. Then*

$$\mathbf{E}\left[\sum_{\mathcal{Y} \subseteq \mathcal{P}_n} h(\mathcal{Y}, \mathcal{P}_n)\right] = \frac{n^k}{k!}\mathbf{E}[h(\mathcal{X}_k, \mathcal{X}_k \cup \mathcal{P}_n)]$$

where the sum on the left side is over all subsets $\mathcal{Y}$ of the random Poisson point set $\mathcal{P}_n$, and on the right side the set $\mathcal{X}_k$ is a binomial process with k nodes, independent of $\mathcal{P}_n$.

We need to estimate the number of subsets with some specified topology, *e.g.*, two nodes are local minima w.r.t. each other. But it is not so easy to estimate this among Poisson point processes. The Palm theory allows us to place a set of random points first and then estimate the expectation over the Poisson point process. This technique will be used in proof of Theorem 7.

4. Delivery guarantee of 3D greedy routing

In this section, we study how to guarantee the packet delivery of 3D greedy routing. We first prove that 3D greedy routing can guarantee the delivery on Delaunay triangulation. Then, we investigate the critical transmission radius of 3D greedy routing in random networks.

4.1. 3D greedy routing on delaunay trianglation

In a d-dimensional Euclidean space, a Delaunay triangulation [32] is a triangulation $Del(V)$ such that there is no point in V inside the circum-hypersphere of any d-simplex in $Del(V)$. For example, in 3D space the 3-simplex is a tetrahedron, while in 2D scarce the 2-simplex is a triangle. In [33], Morin proved that 2D greedy routing can guarantee the packet delivery on Delaunay triangulation. Here, we extend his proof to 3D space.

Theorem 6. *The 3-dimensional greedy routing can guarantee the packet delivery on any Delaunay triangulation Del(V).*

Proof. Assume that t is the destination. We first prove that every node v in $Del(V)$ has a neighbor that is strictly closer to t than v is. In other words, there is no local minimum for 3D greedy routing in $Del(V)$. In Euclidean space, the Delaunay triangulation $Del(V)$ of V corresponds to the dual graph of the Voronoi diagram $Vor(V)$ of V. Let f be the first face in $Vor(V)$ intersected by the directed line from v to t. The face f must exist, since v and t are contained in two different Voronoi cells. See Fig. 3 for illustration. Face f is the boundary shared by two Voronoi cells, one for v and one for some node u. The 2D plane which face f defines partitions the 3D space into two open subspaces (all points in the same subspace with v is closer to v than to u, while all points in the same subspace with u is closer to u than to v). Since t is in the same subspace with u, node u is closer to t than node v. Therefore, at each routing step of 3D greedy routing, the packet gets closer to t. The number of steps is bound by n, thus, the packet is guaranteed to reach t. □

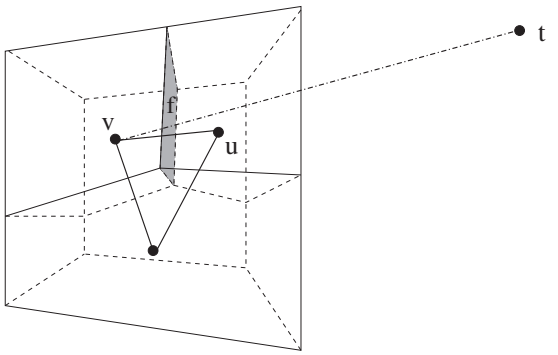

Fig. 3. Any node v can find a neighbor u which is strictly closer to t than v is.

Delaunay triangulation has been used as routing topology for wireless ad hoc networks [34,24]. Since building the Delaunay triangulation needs global information and the length of a Delaunay edge could be longer than the maximum transmission radius, both methods [34,24] use some local structures to approximate the Delaunay triangulation. This can break the delivery guarantee of 3D greedy routing.

4.2. Critical transmission radius of 3D greedy

Next we will prove the following theorem on critical transmission radius $\rho(\mathcal{P}_n)$ of 3D greedy routing in random sensor networks.

Theorem 7. *Let $\beta_0 = 3.2$ and $n(\frac{4}{3}\pi r_n^3) = (\beta + o(1))\ln n$ for some $\beta > 0$. Then, for 3D greedy routing,*

1. *If $\beta > \beta_0$, then $\rho(\mathcal{P}_n) \leqslant r_n$ is* a.a.s.
2. *If $\beta < \beta_0$, then $\rho(\mathcal{P}_n) > r_n$ is* a.a.s.

To simplify the argument, we ignore boundary effects by assuming that there are nodes outside $\mathbb{D}$ with the same distribution. So, if necessary, packets can be routed through those nodes outside $\mathbb{D}$.

4.2.1. Upper bound of Theorem 7

The upper bound in Theorem 7 is going to be proved through a technique called minimal scan statistics. For a finite point set V and a real number $r > 0$, we define

$$S(V, r) = \min_{u,v \in \mathbb{D}, \|u-v\|=r} \#(V \cap L_{uv}).$$

$S(V,r)$ is the minimal number of nodes of V that can be covered by a biconvex with depth r. In other words, $S(V,r)$ is the minimal number of "better" neighboring nodes that any intermediate node u can choose for any possible destination v. As proved in [29], $S(\mathcal{P}_n, r_n) > 0$ implies the event $\rho(\mathcal{P}_n) \leqslant r_n$. Therefore, it suffices to prove that $S(\mathcal{P}_n, r_n) > 0$ is a.a.s. Instead, we now prove a stronger result shown in the following lemma.

Lemma 8. *Suppose that $n(\frac{4}{3}\pi r_n^3) = (\beta + o(1))\ln n$ for some $\beta > \beta_0$. Then for any constant $\beta_1 \in (\beta_0, \beta)$, it is a.a.s. that*

$$S(\mathcal{P}_n, r_n) > \mathcal{L}\left(\frac{\beta_1}{\beta_0}\right)\ln n.$$

Proof. To have the lower bound of minimal scan statistics, we apply the tessellation technique to discretize the scanning process. We tessellate the deployment region by properly choosing cell size such that: (1) each copy of the biconvex contains a polycube with volume at least $\eta\frac{\ln n}{n}$ for some $\eta > 1$, and (2) the number of polycubes is $O(\frac{n}{\ln n})$. Let $d = \sqrt{3}r_n$ which is the largest distance between any two points in a biconvex. For a given β_1, choose a constant $\beta_2 \in (\beta_1,\beta)$, and let $\varepsilon = \frac{4}{27\beta_0}\left(1-\frac{\beta_2}{\beta}\right)$. Consider an ε d-tessellation. (Note that $\varepsilon$is chosen such that each copy of the biconvex contains a polycube with volume at least $\eta\frac{n}{\ln n}$ for some $\eta > 1$.) To prove this inequality, it is sufficient to show that any biconvex of two points in $\mathbb{D}$ that are separated by a distance of r_n contains a polycube with span at most $\frac{1}{\varepsilon}$ and volume at least $\frac{\beta_2}{\beta_0}\left(\frac{4}{3}\pi r_n^3\right)\frac{1}{\beta}$.

For a biconvex L, let P denote the polycube induced by $L_{-\sqrt{3}\varepsilon d}$. Then, $P \subseteq L$, and the span of P is at most $\left\lceil\frac{d-2\sqrt{3}\varepsilon d}{\varepsilon d}\right\rceil + 1 < \frac{1}{\varepsilon}$. By Lemma 2 and the fact that $|L| = \frac{4}{3}\pi r_n^3\frac{1}{\beta_0} = \frac{4}{9\sqrt{3}}\pi d^3\frac{1}{\beta_0}$, we have

$$\begin{aligned}|P| &\geqslant |L_{-\sqrt{3}\varepsilon d}| \geqslant |L| - \pi d^2(\sqrt{3}\varepsilon d) = |L| - \sqrt{3}\varepsilon\pi d^3\\ &= |L| - \frac{27\beta_0}{4}\varepsilon|L| = |L|\left(1-\frac{27\beta_0}{4}\varepsilon\right) = \frac{\beta_2}{\beta}|L|\\ &= \frac{\beta_2}{\beta_0}\left(\frac{4}{3}\pi r_n^3\right)\frac{1}{\beta}.\end{aligned}$$

Let I_n denote the number of polycubes in $\mathbb{D}$ with span at most $\frac{1}{\varepsilon}$ and volume at least $\frac{\beta_2}{\beta_0}\left(\frac{4}{3}\pi r_n^3\right)\frac{1}{\beta} = \left(\frac{\beta_2}{\beta_0}+o(1)\right)\frac{\ln n}{n}$, and Y_i be the number of nodes on the ith polycubes. Then Y_i is a Poisson RV with rate at least $\left(\frac{\beta_2}{\beta_0}+o(1)\right)\ln n$. Since the number of cells in $\mathbb{D}$ is $O\left(\left(\frac{1}{\varepsilon d}\right)^3\right) = O(\frac{n}{\ln n})$, by Lemma 3, $I_n = O(\frac{n}{\ln n})$. By Lemma 4, it is a.a.s. that

$$\frac{\min_{i=1}^{I_n} Y_i}{\ln n} \geqslant \mathcal{L}\left(\frac{\beta_2}{\beta_0}\right) > \mathcal{L}\left(\frac{\beta_1}{\beta_0}\right).$$

Thus,

$$\mathcal{S}(\mathcal{P}_n, r_n) \geqslant \min_{i=1}^{I_n} Y_i > \mathcal{L}\left(\frac{\beta_1}{\beta_0}\right)\ln n. \quad \square$$

4.2.2. Lower bound of Theorem 7

The second half of Theorem 7 can be proved by showing that if $r_n = \sqrt[3]{\frac{3\beta\ln n}{4\pi n}}$ for any $\beta < \beta_0$, there a.a.s. exists local minima. The space is going to be tessellated into equal-size cube cells. For each cell, an event that implies the existence of local minima in the cell is introduced, and a lower bound for the probability of the event is derived. Since these events are identical and independent over cells, we can estimate a probability lower of existence of local minima. By showing the lower bound is a.a.s. equal to 1, we prove the second part of Theorem 7. The detail is given below.

Let β_1 and β_2 be two positive constants such that $\max\left(\frac{1}{8}\beta_0,\beta\right) < \beta_1 < \beta_2 < \beta_0$. In addition, let R_1 and R_2 be given by $n\left(\frac{4}{3}\pi R_1^3\right) = \beta_1\ln n$ and $n\left(\frac{4}{3}\pi R_2^3\right) = \beta_2\ln n$, respectively. Since $\frac{1}{8}\beta_0 < \beta_1 < \beta_2 < \beta_0$, we have $\frac{1}{2}R_2 \leqslant R_1 \leqslant R_2$. Divide $\mathbb{D}$ by $\left(4\sqrt[3]{\frac{\ln n}{n\pi}}\right)$-tessellation. Let I_n denote the number of cells fully contained in $\mathbb{D}$. Here we have $I_n = O(\frac{n}{\ln n})$. For each cell fully contained in $\mathbb{D}$, we draw a ball of radius $\frac{1}{2}\sqrt[3]{\frac{\ln n}{n\pi}}$ at the center of the cell. For $1 \leqslant i \leqslant I_n$, let E_i be the event that there exists two nodes $X, Y \in \mathcal{P}_n$ such that their midpoint is in the ith ball, their distance is between R_1 and R_2, and there is no other node in L_{XY}. For any two nodes u and v with $\|u-v\| > r_n$, if there are no other nodes in L_{uv}, u and v are local minima w.r.t. each other. So, E_i implies existence of local minimum, and

$$\Pr[\rho(\mathcal{P}_n) > r_n] \geqslant \Pr[\text{at least one } E_i \text{ occurs}].$$

Let o_i denote the center of the ith ball, and u,v be two points such that $\frac{1}{2}(u+v)$ is in the ith ball and $R_1 \leqslant \|u-v\| \leqslant R_2$. By triangle inequality, for any point $w \in L_{uv}$, we have $\|w-o_i\| \leqslant \|w-\frac{1}{2}(u+v)\| + \|o_i-\frac{1}{2}(u+v)\| < \frac{\sqrt{3}}{2}\sqrt[3]{\frac{3\beta_0\ln n}{4n\pi}} + \frac{1}{2}\sqrt[3]{\frac{\ln n}{n\pi}} < 2\sqrt[3]{\frac{\ln n}{n\pi}}$. Since the width of cells is $4\sqrt[3]{\frac{\ln n}{n\pi}}$, u, v, and L_{uv} are contained in the ith cube. Therefore, $E_1,\ldots,E_{I_i}$ are independent. In addition, $E_1,\ldots,E_{I_i}$ are identical. Then,

$$\Pr[\text{none of } E_i \text{ occurs}] = (1-\Pr[E_1])^{I_n} \leqslant e^{-I_n\Pr(E_1)}.$$

If $I_n\Pr(E_1) \to \infty$, we may have $\Pr[\rho(\mathcal{P}_n) > r_n] \to 1$ and the second half of Theorem 7 follows. Next, we will prove that $I_n\Pr(E_1) \to \infty$.

First, we introduce several relevant events and derive their probabilities. Let A denote the disk with radius $\frac{1}{2}\sqrt[3]{\frac{\ln n}{n\pi}}$ at the center of the first cube. Assume V is a point set and $T \subset V$. Let $h_1(T,V)$ denote a function such that $h_1(T=\{x_1,x_2\},V)=1$ only if $\frac{1}{2}(x_1+x_2) \in A, R_1 \leqslant \|x_1-x_2\| \leqslant R_2$, and there is no other node of V in $L_{x_1x_2}$; otherwise, $h_1(T,V)=0$. In addition, under Boolean addition, for any $\{x_1,x_2,x_3\} \subseteq V$, let $h_2(\{x_1,x_2,x_3\},V) = h_1(\{x_1,x_2\},V)\times h_1(\{x_1,x_3\},V) + h_1(\{x_2,x_1\},V)\times h_1(\{x_2,x_3\},V) + h_1(\{x_3,x_1\},V)\times h_1(\{x_3,x_2\},V)$; for any $\{x_1,x_2,x_3,x_4\} \subseteq V$, let $h_3(\{x_1,x_2,x_3,x_4\},V) = h_1(\{x_1,x_2\},V)\times h_1(\{x_3,x_4\},V) + h_1(\{x_1,x_3\},V)\times h_1(\{x_2,x_4\},V) + h_1(\{x_1,x_4\},V)\times h_1(\{x_2,x_3\},V)$. E_1 is the event that there exists two nodes $X, Y \in \mathcal{P}_n$ such that $h_1(\{X,Y\},\mathcal{P}_n) = 1$. In the remaining of this subsection, we use X_1', X_2', X_3' and X_4' to denote elements of $\mathcal{P}_n$. Let $F_1'(\{X_1',X_2'\})$ be the event that $h_1(\{X_1',X_2'\},\mathcal{P}_n) = 1$; $F_2'(\{X_1',X_2',X_3'\})$ be the event that $h_2(\{X_1',X_2',X_3'\},\mathcal{P}_n)=1$; and $F_3'(\{X_1',X_2',X_3',X_4'\})$ be the event that $h_3(\{X_1',X_2',X_3',X_4'\},\mathcal{P}_n)=1$. Applying Boole's inequalities, we have

$$\begin{aligned}\Pr[E_1] \geqslant &\sum_{\{X_1',X_2'\}\subseteq\mathcal{P}_n}\Pr[F_1'(\{X_1',X_2'\})]\\ &-\sum_{\{X_1',X_2',X_3'\}\subseteq\mathcal{P}_n}\Pr[F_2'(\{X_1',X_2',X_3'\})]\\ &-\sum_{\{X_1',X_2',X_3',X_4'\}\subseteq\mathcal{P}_n}\Pr[F_3'(\{X_1',X_2',X_3',X_4'\})]. \qquad (2)\end{aligned}$$

For the sake of clarity, we use X_1,X_2,X_3 and X_4 to denote independent random points with uniform distribution over $\mathbb{D}$ and independent of $\mathcal{P}_n$. Let F_1 be the event that $h_1(\{X_1,X_2\},\{X_1,X_2\}\cup\mathcal{P}_n)=1$, F_2 be the event that $h_2(\{X_1,X_2,X_3\},\{X_1,X_2,X_3\}\cup\mathcal{P}_n)=1$, and F_3 be the event that $h_3(\{X_1,X_2,X_3,X_4\},\{X_1,X_2,X_3,X_4\}\cup\mathcal{P}_n)=1$. According to the Palm theory (Theorem 5), we have

$$\sum_{\{X_1',X_2'\}\subseteq\mathcal{P}_n}\Pr[F_1'(\{X_1',X_2'\})]=\mathbf{E}\left[\sum_{\{X_1',X_2'\}\subseteq\mathcal{P}_n}h_1(\{X_1',X_2'\},\mathcal{P}_n)\right]$$
$$=\frac{n^2}{2!}\mathbf{E}[h_1(\{X_1,X_2\},\{X_1,X_2\}\cup\mathcal{P}_n)]$$
$$=\frac{n^2}{2}\Pr[F_1];\tag{3}$$

$$\sum_{\{X_1',X_2',X_3'\}\subseteq\mathcal{P}_n}\Pr[F_2'(\{X_1',X_2',X_3'\})]$$
$$=\mathbf{E}\left[\sum_{\{X_1',X_2',X_3'\}\subseteq\mathcal{P}_n}h_2(\{X_1',X_2',X_3'\},\mathcal{P}_n)\right]$$
$$=\frac{n^3}{3!}\mathbf{E}[h_2(\{X_1,X_2,X_3\},\{X_1,X_2,X_3\}\cup\mathcal{P}_n)]$$
$$=\frac{n^3}{2}\Pr[F_2];\tag{4}$$

and

$$\sum_{\{X_1',X_2',X_3',X_4'\}\subseteq\mathcal{P}_n}\Pr[F_3'(\{X_1',X_2',X_3',X_4'\})]$$
$$=\mathbf{E}\left[\sum_{\{X_1',X_2',X_3',X_4'\}\subseteq\mathcal{P}_n}h_3(\{X_1',X_2',X_3',X_4'\},\mathcal{P}_n)\right]$$
$$=\frac{n^4}{4!}\mathbf{E}[h_3(\{X_1,X_2,X_3,X_4\},\{X_1,X_2,X_3,X_4\}\cup\mathcal{P}_n)]$$
$$=\frac{n^4}{8}\Pr[F_3].\tag{5}$$

From Eqs. (2)–(5), we have

$$\Pr[E_1]\geqslant\frac{n^2}{2}\Pr[F_1]-\frac{n^3}{2}\Pr[F_2]-\frac{n^4}{8}\Pr[F_3].\tag{6}$$

In the next, we will derive the probabilities of F_1, F_2, and F_3. Let S_1 denote the set $\{(x_1,x_2)|\frac{1}{2}(x_1+x_2)\in A, R_1\leqslant\|x_1-x_2\|\leqslant R_2.\}$. We have

$$\Pr[F_1]=\iint_{S_1}\Pr[F_1|X_1=x_1,X_2=x_2]\,dx_1dx_2$$
$$=\iint_{S_1}e^{-n|L_{x_1x_2}|}dx_1dx_2=\iint_{S_1}e^{-n\frac{1}{\beta_0}(\frac{4}{3}\pi\|x_1-x_2\|^3)}dx_1dx_2.$$

Let $z=\frac{x_1+x_2}{2}$ and $r=\frac{1}{2}\|x_1-x_2\|$. Then,

$$\Pr[F_1]=\int_{z\in A}\int_{r=\frac{R_1}{2}}^{\frac{R_2}{2}}e^{-\frac{n}{\beta_0}\frac{32}{3}\pi r^3}32\pi r^2drdz$$
$$=\int_{z\in A}\int_{r=\frac{R_1}{2}}^{\frac{R_2}{2}}e^{-\frac{n}{\beta_0}\frac{32}{3}\pi r^3}d\left(\frac{32}{3}\pi r^3\right)dz$$
$$=-\left(\frac{\beta_0}{n}e^{-\frac{n}{\beta_0}\frac{32}{3}\pi r^3}\Big|_{r=\frac{R_1}{2}}^{\frac{R_2}{2}}\right)|A|$$
$$=\frac{\beta_0}{6n^2}\left(n^{-\frac{\beta_1}{\beta_0}}-n^{-\frac{\beta_2}{\beta_0}}\right)\ln n.\tag{7}$$

Let S_2 denote the set $\left\{(x_1,x_2,x_3)\middle|\begin{array}{l}\frac{x_1+x_2}{2},\frac{x_1+x_3}{2}\in A;\\ R_1\leqslant\|x_1-x_2\|\leqslant R_2; x_1,x_2\notin L_{x_1x_3};\\ R_1\leqslant\|x_1-x_3\|\leqslant R_2; x_1,x_3\notin L_{x_1x_2}\end{array}\right\}$.

Applying Lemma 1, if $(x_1,x_2,x_3)\in S_2$, we have

$$\Pr[F_2]=\iiint_{S_2}\Pr\left[F_2\middle|\begin{array}{c}X_i=x_i\\ \forall i=1,2,3\end{array}\right]dx_1dx_2dx_3$$
$$\leqslant 3\iiint_{S_2}e^{-n|L_{x_1x_2}\cup L_{x_1x_3}|}dx_1dx_2dx_3$$
$$\leqslant 3\iiint_{S_2}e^{-n\left(\frac{1}{\beta_0}\frac{4}{3}\pi\|x_1-x_2\|^3+\gamma R_2^2\left\|\frac{x_1+x_2}{2}-\frac{x_1+x_3}{2}\right\|\right)}\cdot dx_1dx_2dx_3.$$

Let $z_1=\frac{x_1+x_2}{2}, z_2=\frac{x_1+x_3}{2}, r=\frac{\|x_1-x_2\|}{2}$, and $\rho=\|z_1-z_2\|$. Then,

$$\Pr[F_2]\leqslant 3\int_{z_1\in A}\int_{r=\frac{R_1}{2}}^{\frac{R_2}{2}}\int_{z_2\in A}e^{-n\left(\frac{1}{\beta_0}\frac{32}{3}\pi r^3+\gamma R_2^2\|z_1-z_2\|\right)}\cdot 256\pi r^2drdz_1dz_2$$
$$\leqslant 24\int_{z_1\in A}\int_{r=\frac{R_1}{2}}^{\frac{R_2}{2}}e^{-\frac{n}{\beta_0}\left(\frac{32}{3}\pi r^3\right)}d\left(\frac{32}{3}\pi r^3\right)dz_1\cdot\int_{z_2\in A}e^{-\gamma nR_2^2\|z_1-z_2\|}dz_2$$
$$\leqslant 24\int_{z_1\in A}\int_{r_1=\frac{R_1}{2}}^{\frac{R_2}{2}}e^{-\frac{n}{\beta_0}\left(\frac{32}{3}\pi r^3\right)}d\left(\frac{32}{3}\pi r^3\right)dz_1\cdot\int_{\rho=0}^{\infty}e^{-\gamma nR_2^2\rho}4\pi\rho^2d\rho$$
$$=24\left(\frac{\beta_0}{6n^2}\left(n^{-\frac{\beta_1}{\beta_0}}-n^{-\frac{\beta_2}{\beta_0}}\right)\ln n\right)\left(\frac{8\pi}{\left(\gamma nR_2^2\right)^3}\right)$$
$$=\frac{32\pi\beta_0}{\gamma^3\left(nR_2^3\right)^2n^3}\left(n^{-\frac{\beta_1}{\beta_0}}-n^{-\frac{\beta_2}{\beta_0}}\right)\ln n.\tag{8}$$

Let S_3 denote the set $\left\{(x_1,x_2,x_3,x_4)\middle|\begin{array}{l}\frac{x_1+x_2}{2},\frac{x_3+x_4}{2}\in A;\\ R_1\leqslant\|x_1-x_2\|\leqslant R_2; x_1,x_2\notin L_{x_3x_4};\\ R_1\leqslant\|x_3-x_4\|\leqslant R_2; x_3,x_4\notin L_{x_1x_2}\end{array}\right\}$.

Applying Lemma 1, if $(x_1,x_2,x_3,x_4)\in S_3$, we have

$$\Pr[F_3]=\iint\iint_{S_3}\Pr\left[F_3\middle|\begin{array}{c}X_i=x_i,\\ \forall i=1,2,3,4\end{array}\right]dx_1dx_2dx_3dx_4$$
$$\leqslant 3\iint\iint_{S_3}e^{-n|L_{x_1x_2}\cup L_{x_3x_4}|}dx_1dx_2dx_3dx_4$$
$$\leqslant 3\iint\iint_{S_3}e^{-n\left(\frac{1}{\beta_0}\frac{4}{3}\pi\|x_1-x_2\|^3+\gamma R_2^2\left\|\frac{x_1+x_2}{2}-\frac{x_3+x_4}{2}\right\|\right)}\cdot dx_1dx_2dx_3dx_4.$$

Let $z_1=\frac{x_1+x_2}{2}, r_1=\frac{\|x_1-x_2\|}{2}, z_2=\frac{x_3+x_4}{2}, r_2=\frac{\|x_3-x_4\|}{2}$, and $\rho=\|z_1-z_2\|$. Then, Pr $[F_3]$

$$\leqslant 3\int_{z_1\in A}\int_{r_1=\frac{R_1}{2}}^{\frac{R_2}{2}}\int_{z_2\in A}\int_{r_2=\frac{R_1}{2}}^{\frac{R_2}{2}} e^{-n\left(\frac{1}{\beta_0}\frac{32}{3}\pi r_1^3+\gamma R_2^2\|z_1-z_2\|\right)} \cdot (32\pi r_1^2 dr_1 dz_1)(32\pi r_2^2 dr_2 dz_2)$$

$$\leqslant 3\left(\int_{z_1\in A}\int_{r_1=\frac{R_1}{2}}^{\frac{R_2}{2}} e^{-\frac{n}{\beta_0}\frac{32}{3}\pi r_1^3} d\left(\frac{32}{3}\pi r^3\right)dz\right) \cdot \left(32\pi\left(\frac{R_2}{2}\right)^2\left(\frac{R_2}{2}-\frac{R_1}{2}\right)\int_{\rho=0}^{\infty} e^{-\gamma n R_2^2\rho} 4\pi\rho^2 d\rho\right)$$

$$= \frac{16\pi^2\beta_0}{\gamma^3\left(nR_2^3\right)n^4}\left(1-\frac{R_1}{R_2}\right)\left(n^{-\frac{\beta_1}{\beta_0}}-n^{-\frac{\beta_2}{\beta_0}}\right)\ln n. \quad (9)$$

Put Eqs. (6)–(8) together. We have

$$\Pr[E_1] \geqslant \left(\frac{\beta_0}{12}-\frac{16\pi\beta_0}{\gamma^3\left(nR_2^3\right)^2}-\frac{2\pi^2\beta_0}{\gamma^3\left(nR_2^3\right)}\left(1-\frac{R_1}{R_2}\right)\right) \cdot \left(n^{-\frac{\beta_1}{\beta_0}}-n^{-\frac{\beta_2}{\beta_0}}\right)\ln n \sim \frac{\beta_0}{12}\left(n^{-\frac{\beta_1}{\beta_0}}-n^{-\frac{\beta_2}{\beta_0}}\right)\ln n.$$

Since $I_n=\Omega(\frac{\ln n}{n})$, we have $\Pr[E_1]=\Omega\left(\left(n^{-\frac{\beta_1}{\beta_0}}-n^{-\frac{\beta_2}{\beta_0}}\right)\ln n\right)$, and

$$I_n\Pr[E_1]=\Omega\left(n^{1-\frac{\beta_1}{\beta_0}}\right)\to\infty.$$

This complete the proof of the second half of Theorem 7.

5. Energy-efficiency of 3D greedy routing

Since Flury and Wattenhofer [2] showed *no* deterministic localized routing protocol is energy-efficient in 3D networks, the simple 3D greedy routing may lead to energy-inefficient paths in the worst case. Therefore, we are interested in designing a localized routing method that is energy-efficient with high probability for random 3D networks. Here a routing method is energy-efficient with high probability if (1) with high probability, the routing method will find a path successfully; and (2) with high probability, the found path is energy-efficient.

5.1. Energy-efficient restricted 3D greedy routing (ERGrd)

Our energy-efficient localized 3D routing method is a variation of classical 3D greedy routing and an extension of a localized routing method [13] we designed for 2D networks. In 3D greedy routing, current node u selects its next hop neighbor based purely on its distance to the destination, i.e., it sends the packet to its neighbor who is closest to the destination. However, such choice might not be the most energy-efficient link locally, and the overall route might not be globally energy-efficient too. Therefore, our routing method use two concepts *energy mileage* and *restricted region* to refine the choices of forwarding nodes in 3D greedy routing.

Energy mileage. Given a energy model $\mathbf{e}(x)$, *energy mileage* is the ratio between the transmission distance and the energy-consumption of such transmission, *i.e.*, $\frac{x}{\mathbf{e}(x)}$. Let $\mathbf{r}_0$ be the value such that $\frac{\mathbf{r}_0}{\mathbf{e}(\mathbf{r}_0)}=\max_x\frac{x}{\mathbf{e}(x)}$. We call $\mathbf{r}_0$ as the *maximum energy mileage distance*[1] under energy model $\mathbf{e}(x)$. We assume that the energy mileage $\frac{x}{\mathbf{e}(x)}$ is an increasing function when $x<\mathbf{r}_0$ and a decreasing function when $x>\mathbf{r}_0$. This assumption is true for most of commonly used energy models. For example, if $\mathbf{e}(\|uv\|)=\|uv\|^2+c$ is the energy used by sending message from u to v, the maximum energy mileage distance $\mathbf{r}_0=\sqrt{c}$. Our 3D localized routing greedily selects the neighbor who can maximize the energy mileage as the forwarding node.

Restricted region. Instead of selecting the forwarding node from all neighbors of current node u (a unit ball in 3D as shown in Fig. 4a), our 3D routing method prefers the forwarding node v inside a smaller restricted region. The region is defined inside a 3D cone with an angle parameter $\alpha<\pi/3$, such that angle $\angle vut\leqslant\alpha$, as shown in Fig. 4b. The use of α (restricting the forwarding direction) is to bound the total distance of the routing path. Then the restricted region is a region inside this 3D cone and near the maximum energy mileage distance $\mathbf{r}_0$, such that every node v inside this area satisfies $\eta_1\mathbf{r}_0\leqslant\|uv\|\leqslant\eta_2\mathbf{r}_0$, as shown in Fig. 4b. Here, η_1 and η_2 are two constant parameters. This can help us to prove the energy-efficiency of the route.

Notice that both these ideas are not completely new. Restricted region with an angle has been used in some localized routing methods, such as nearest/farthest neighbor routing [34], while concepts similar to energy mileage have been used in some energy-aware localized routing methods [11,12,35]. However, combining both of these techniques to guarantee energy-efficiency is first done in our previous work [13] for 2D networks. In this paper, we further adapt them into 3D routing.

Our energy-efficient localized 3D routing protocol is given in Algorithm 1. There are four parameters used by our method. Three adjustable parameters $0<\alpha<\frac{\pi}{3}$ and $\eta_1<1<\eta_2$ define the restricted region, while $\mathbf{r}_0$ is the best energy mileage distance based on the energy model. For example, the following setting of these parameters can be used for energy model $\mathbf{e}(x)=x^2+c:\alpha=\frac{\pi}{4},\mathbf{r}_0=\sqrt{c}$, $\eta_1=1/2$ and $\eta_2=2$. Hereafter, we denote the routing algorithm, *energy-efficient restricted greedy*, as ERGrd if *no* greedy routing (Grd) is used when no node v satisfies that $\angle vut\leqslant\alpha$. If Grd is applied afterward, then the routing protocol is denoted ERGrd+Grd. Notice that if Grd fails to find a forwarding node, randomized scheme [2] could also be applied.

The path efficiency of 3D ERGrd is given by the following two theorems. The detail proofs of these two theorems

[1] Here, we assume that $d\left(\frac{\mathbf{e}(x)}{x}\right)/dx$ is monotone increasing, thus, $\mathbf{r}_0$ is unique.

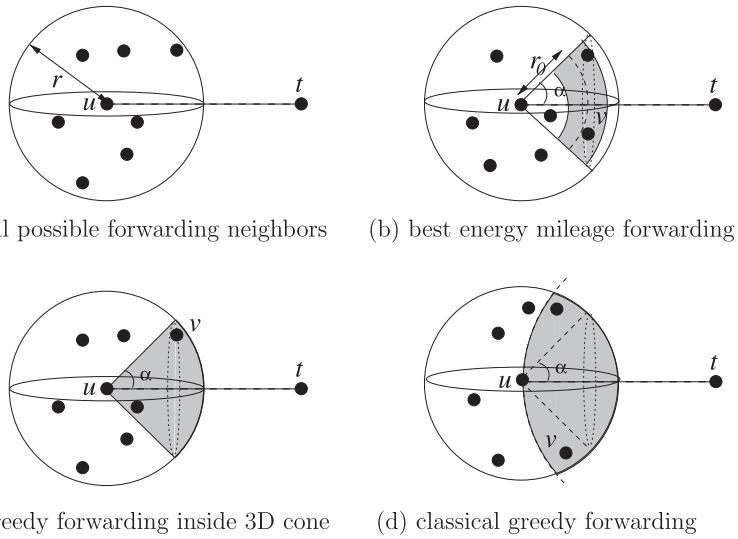

Fig. 4. Illustrations of our 3D routing: (a) energy-efficient forwarding in the restricted region, (b) greedy forwarding in the 3D cone, (c) greedy forwarding when the 3D cone is empty.

are exactly the same with the proofs of Theorems 1–3 in [13] for 2D network, thus are ignored here.

Theorem 9. *When 3D ERGrd routing indeed finds a path* $\mathbf{P}_{ERGrd}(s,t)$ *from the source s to the target t, the total Euclidean length of the found path is at most* $\delta\|t-s\|$ *where* $\delta = \frac{1}{1-2\sin\frac{\alpha}{2}}$, *thus, a constant factor of the optimum.*

Theorem 10. *When 3D ERGrd routing indeed finds a path* $\mathbf{P}_{ERGrd}(s,t)$ *from the source s to the target t, the total energy-consumption of the found path is within a constant factor* σ *of the optimum. When* $\mathbf{r}_0 \geqslant r$, σ *depends on* α; *otherwise, depends on* η_1, η_2 *and* α.

Algorithm 1. Energy-efficient restricted 3D greedy routing (3D ERGrd)

while node u receives a packet with destination t **do**
  if t is a neighbor of u **then**
    Node u forwards the packet to t directly.
  else if there are neighbors inside the restricted region and $\mathbf{r}_0 < r$ **then**
    Node u forwards the packet to the neighbor v such that its energy mileage $\frac{\|uv\|}{\mathbf{e}(\|uv\|)}$ is maximum among all neighbors w inside the restricted region, as shown in Fig. 4b.
  else if there are neighbors inside the 3D cone **then**
    Node u finds the node v inside the 3D cone (Fig. 4c) with the minimum $\|t-v\|$.
  else
    Greedy routing (Fig. 4d) is applied, or the packet is simply dropped.
  end if
end while

5.2. Critical transmission radius of 3D ERGrd

Notice that 3D ERGrd routing may fail, as all other greedy-based methods do, when an intermediate node cannot find a better neighbor to forward the packet. We now study the critical transmission radius for ERGrd routing in random 3D wireless networks. Given a set of nodes V distributed in a region $\mathbb{D}$, the critical transmission radius $\rho(V)$ for successful routing by 3D ERGrd is

$$\max_{u,v} \min_{w:\angle wuv \leqslant \alpha} \|w-u\|. \tag{10}$$

By setting the $r = \rho(V)$, ERGrd can always find a forwarding node inside the 3D cone region, thus can guarantee its packet delivery. Now, we can prove a similar result for 3D ERGrd as we did for 3D greedy routing.

Theorem 11. *Let* $\beta_0 = \frac{2}{1-\cos\alpha}$ *and* $n(\frac{4}{3}\pi r_n^3) = \beta \ln n$ *for some* $\beta > 0$. *Then, for 3D ERGrd routing,*

1. *If* $\beta > \beta_0$, *then* $\rho(\mathcal{P}_n) \leqslant r_n$ *is a.a.s.*
2. *If* $\beta < \beta_0$, *then* $\rho(\mathcal{P}_n) > r_n$*is a.a.s.*

Here, $\beta_0 = \frac{4\pi/3}{2\pi(1-\cos\alpha)/3} = \frac{2}{1-\cos\alpha}$ is the ratio between the volume of a unit ball and the volume of a 3D cone (the forwarding region) inside the ball. Next, we present the detailed proofs for two parts of this theorem. Again, we ignore boundary effects.

5.2.1. Upper bound of Theorem 11

The proof of this part is very similar to the proof in Theorem 7, we also prove it by proving a lemma similar to Lemma 8 except for $\beta_0 = \frac{2}{1-\cos\alpha}$ now.

Given a node u, the region that node u can choose its neighbor to forward data is a 3D cone with angle 2α, as shown in Fig. 4c. Now L denotes this 3D cone instead of the biconvex. Let d be its diameter (*i.e.*, the largest distance between any two points inside it). Clearly $d = r_n$ when

$\alpha \leqslant \frac{\pi}{6}$, and $d = 2\sin\alpha \cdot r_n$ when $\frac{\pi}{6} \leqslant \alpha < \frac{\pi}{3}$. Thus, $d < \sqrt{3} r_n$. Again the same tessellation technique can be used. The only difference is that $|L| = \frac{4}{3}\pi r_n^3 \frac{1}{\beta_0} > \frac{4}{9\sqrt{3}}\pi d^3 \frac{1}{\beta_0}$ instead of $= \frac{4}{9\sqrt{3}}\pi d^3 \frac{1}{\beta_0}$. However, this will not affect the proof of $|P| > \frac{\beta_2}{\beta_0}\left(\frac{4}{3}\pi r_n^3\right)\frac{1}{\beta}$. The remaining parts are the same with the proof of Lemma 8.

5.2.2. Lower bound of Theorem 11

We now show that, if $r_n = \sqrt[3]{\frac{3\beta \ln n}{4\pi n}}$ for any $\beta < \beta_0$, *a.a.s.*, there are two nodes u and v such that we cannot find a node w for forwarding by node u, *i.e.*, there does not exist node w inside the 3D cone. Again we partition the space using equal-size cubes (called cells) with side-length ηr_n for a constant $0 < \eta$ to be specified later. Thus the number of cells, denoted by I_n here, that are fully contained inside the compact and convex region $\mathbb{D}$ with unit-volume, is $\Theta\left(\frac{1}{\eta^3 r_n^3}\right) = \Theta\left(\frac{n}{\ln n}\right)$. Let $E_{u,v}$ denote the event that no forwarding node w (in the 3D cone) exists for node u to reach node v. Then to prove our claim, it is equivalent to prove that the probability of at least one of the event $E_{u,v}$ happens *a.a.s.*, *i.e.*, 1-**Pr** (none of event $E_{u,v}$ happens). Since the events $E_{u,v}$ are not independent for all pairs u and v, we will only consider a special subset of events that are independent. Consider any cell produced by the 3D grid partition that are contained inside $\mathbb{D}$. For each cell, we draw a shaded cube with side-length $(\eta - 2(1+\delta))r_n$ and it is of distance $(1+\delta)r$ to the boundary of the cell, as shown in Fig. 5a. We only consider the case when node u is located in this shaded cube. We also restrict the node v to satisfy that $r_n < \|u - v\| \leqslant (1+\delta)r_n$, *i.e.*, in the torus region in Fig. 5b. Clearly, node v will also be inside this cell, and the shaded 3D cone where the possible forwarding node could locate is also inside this cell. Thus, events E_{u_1,v_1} and E_{u_2,v_2} are independent if u_1 and u_2 are selected as above from different cells.

For each cell i, we compute the probability that event E_{u_i,v_i} happens, where u_i is selected from the shaded cube of cell i and v_i is selected such that $r_n < \|v_i - u_i\| \leqslant (1+\delta)r_n$. Recall that for any region A, the probability that it is empty of any nodes is $e^{-n|A|}$. Clearly, the probability that node u_i exists is $1 - e^{-n(\eta-2-2\delta)^3 r_n^3}$ since the shared cube has volume $(\eta - 2 - 2\delta)^3 r_n^3$; the probability that node v_i exists is $1 - e^{-n\frac{4}{3}\pi((1+\delta)^3-1)r_n^3}$ since the torus has volume $\frac{4}{3}\pi((1+\delta)^3 - 1)r_n^3$. Given node u_i and v_i, the probability that event E_{u_i,v_i} happens is $e^{-n\frac{2}{3}\pi(1-\cos\alpha)r_n^3} = e^{-\beta/\beta_0 \ln n} = n^{-\beta/\beta_0}$. Consequently, event $E_{u,v}$ happens for some node pairs u_i and v_i is $\mathbf{Pr}(E_{u_i,v_i}) \geqslant \left(1 - e^{-n(\eta-2-2\delta)^3 r_n^3}\right)\left(1 - e^{-n\frac{4}{3}\pi((1+\delta)^3-1)r_n^3}\right)n^{-\beta/\beta_0} = (1 - n^{-\beta(\eta-2-2\delta)^3 3/4\pi})(1 - n^{-\beta((1+\delta)^3-1)})$ $n^{-\beta/\beta_0}$. Thus, the probability that ERGrd routing fails to find a path for some source/destination pairs is **Pr** (at least one of events $E_{u,v}$ happens) $\geqslant$**Pr** (at least one of E_{u_i,v_i} happens)= 1-**Pr** (none of E_{u_i,v_i} happens)= $1 - (1 - \mathbf{Pr}(E_{u_i,v_i}))^{I_n} = 1 - e^{I_n \cdot \ln(1-\mathbf{Pr}(E_{u_i,v_i}))} \geqslant 1 - e^{-I_n \cdot \mathbf{Pr}(E_{u_i,v_i})}$. Notice that $I_n \cdot \mathbf{Pr}(E_{u_i,v_i}) \geqslant \Theta\left(\frac{n}{\ln n}\right)(1 - n^{-\beta(\eta-2-2\delta)^3 3/4\pi})(1 - n^{-\beta((1+\delta)^3-1)})n^{-\beta/\beta_0} \simeq \frac{n^{1-\beta/\beta_0}}{\ln n}$, which goes to ∞ as $n \to \infty$ when $\beta < \beta_0$, $\eta - 2 - 2\delta > 0$, and $\delta > 0$. This can be easily satisfied, *e.g.*, $\delta = 1$, $\eta = 5$. Thus, $\lim_{n\to\infty} 1 - e^{-I_n \cdot \mathbf{Pr}(E_{u_i,v_i})} = 1$. This completes the proof.

6. Simulation

6.1. Critical transmission radius for random networks

We have analyzed the theoretical bounds of the critical transmission radius for 3D greedy routing and 3D ERGrd routing. To confirm our theoretical analysis, we conduct several simulations to see what is the practical value of transmission radius r_n such that greedy can guarantee the packet delivery with high probability in random networks. We randomly generate 1000 networks with n nodes in a $100 \times 100 \times 100$ cubic region, where n is from 50 to 500. For each network V, we compute the critical transmission radius $\rho(V)$ of 3D greedy and 3D ERGrd by their definitions (Eqs. (1) and (10)). For 3D ERGrd routing, we let $\alpha = \pi/6$ or $\alpha = \pi/4$. Fig. 6 gives the histograms of the distribution of $\rho(V)$ of these 3D greedy routing methods for 1000 random networks. Fig. 7 show the probability distribution function of $\rho(V)$ for these methods. It is clear that the CTRs of all methods satisfy a transition phenomena, *i.e.*, there is a radius r_0 such that 3D Grd/ERGrd can successfully deliver all packets when $r_n > r_0$ and cannot deliver some packets when $r_n < r_0$. Notice that the transition becomes faster

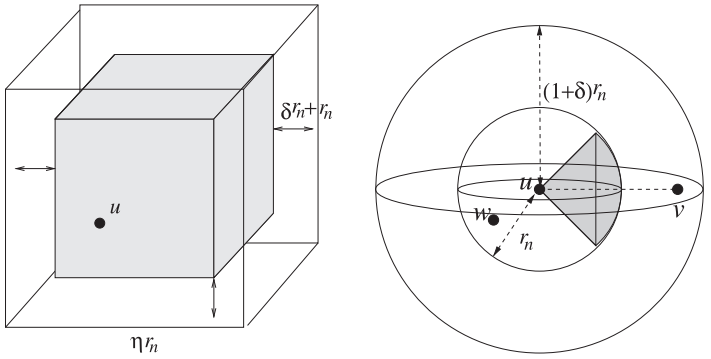

(a) selection of u (b) no forwarding node

Fig. 5. Illustrations of the proof of lower bound: (a) a cubic cell and the region where we select a node u; (b) the event that node u cannot find a forwarding node w to reach a node v.

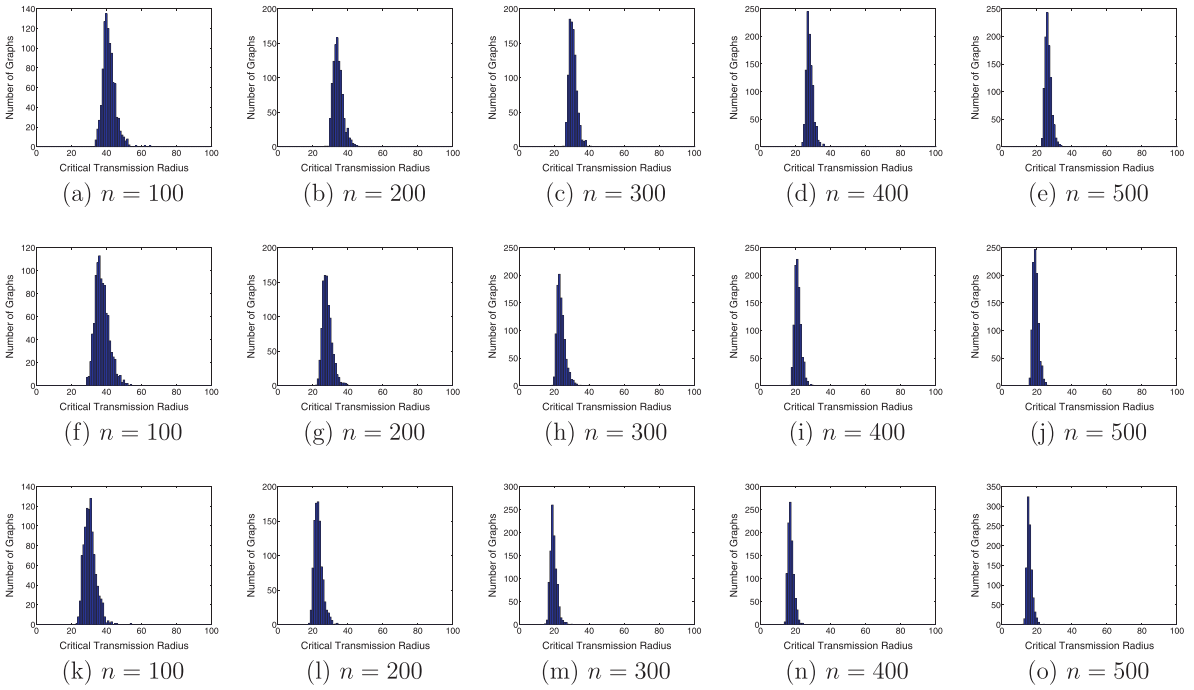

Fig. 6. The distributions of $\rho(V)$ for random networks with 100–500 nodes. (a–e) For 3D greedy, (f–j) for 3D ERGrd with $\alpha = \pi/6$, and (k–o) for 3D ERGrd with $\alpha = \pi/4$.

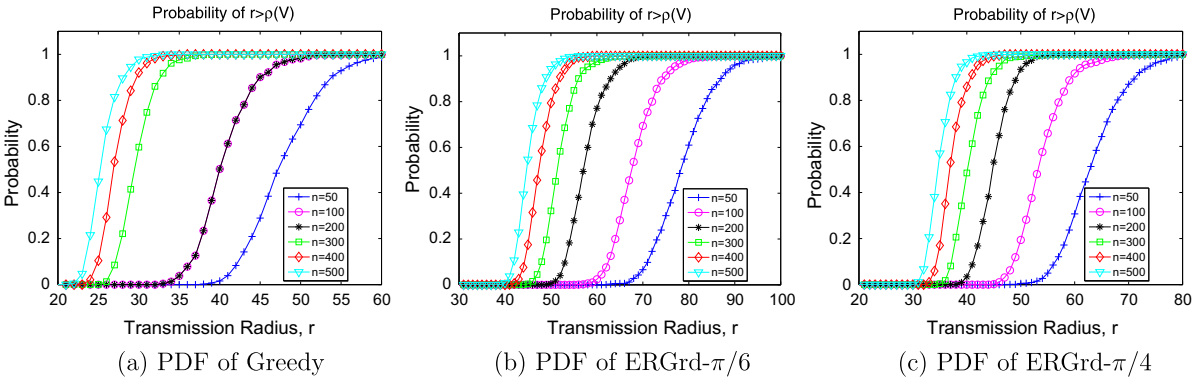

Fig. 7. PDF curves of 3D greedy routing and 3D ERGrd routing with $\alpha = \pi/6$ or $\pi/4$.

when the number of nodes increases. This confirms our theoretical analysis on the existence of CTR. In addition, from these figures, we can find that larger node density always leads to smaller value of CTR. The practical value of $\rho(V)$ is larger than the theoretical bound in our analysis, since the theoretical bound is standing for $n \to \infty$. However, the practical value will approach the theoretical bound with the increasing of n . For example, when $n = 500$, the theoretical bound of 3D greedy is $\sqrt[3]{\frac{3\beta_0 \ln n}{4\pi n}} \times 100 = 0.212 \times 100 = 21.2$ for a $100 \times 100 \times 100$ cubic region. From Fig. 7a, the CTR of 3D greedy is around 25, which already becomes very near the theoretical bound. . Compared the two cases of ERGrd method with $\alpha = \pi/6$ and $\pi/4$, larger CTR is required if smaller restricted region (*i.e.* smaller α) is applied.

6.2. Network performance of 3D greedy routing

We also study network performance of 3D greedy routing and proposed ERGrd routing in random 3D networks via extensive simulation. We implement the classic 3D greedy routing (Grd) and variations of our proposed restricted greedy routing (specifically, ERGrd with $\alpha = \pi/6$, ERGrd with $\alpha = \pi/4$, ERGrd+Grd with $\alpha = \pi/6$, and ERGrd+Grd with $\alpha = \pi/4$) in our simulator. We assume that the energy-consumption of a link uv is $\mathbf{e}(\|uv\|) = \|uv\|^2 + c$, where $c = r^2/4$. The values of η_1 and η_2 are 1/2 and 2. By setting various transmission radii, we generate random networks with 100 wireless nodes again in a $100 \times 100 \times 100$ cubic region. Fig. 8 shows a set of random networks generated on the same set of nodes. We select 100

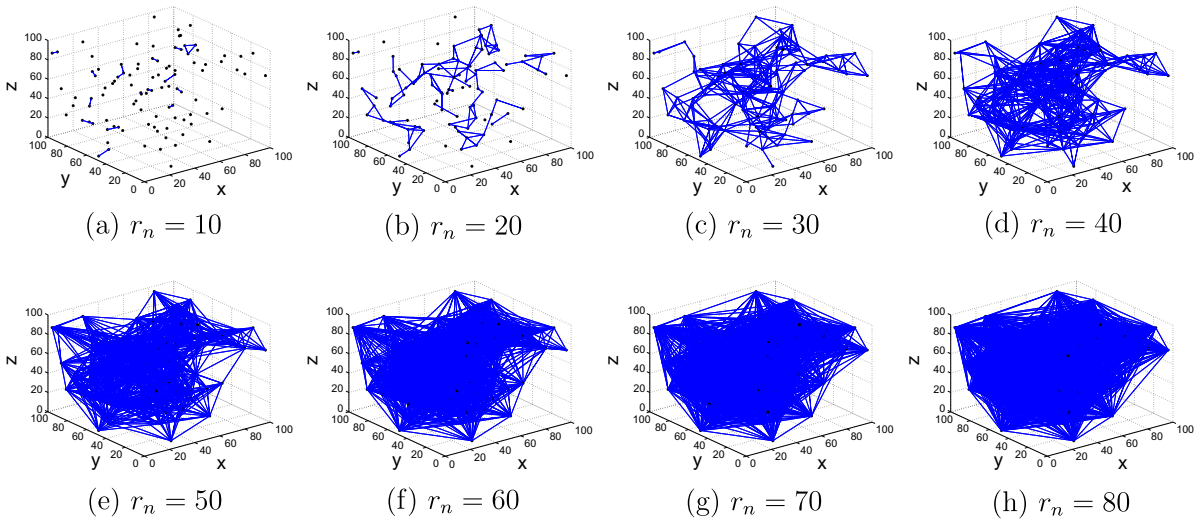

Fig. 8. Network topologies with 100 nodes when r_n is from 10 to 80.

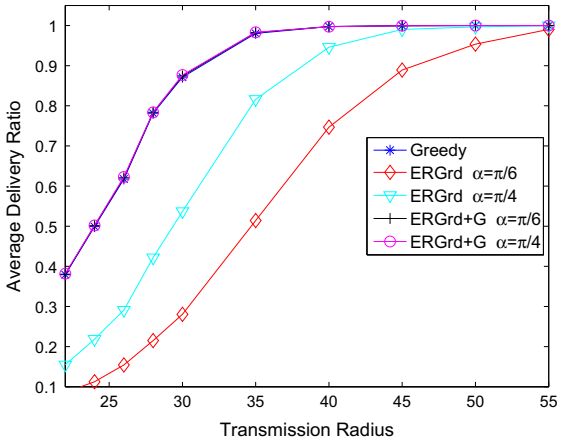

Fig. 9. Average delivery ratios of 3D greedy and 3D ERGrd in random networks.

connected random networks for each setting, then for each network we randomly select 100 source–destination pairs and test five greedy-based 3D routing. All results presented hereafter are average values over all routes and networks. In all figures, ERGrd+G denotes ERGrd+Grd, which is the restricted greedy routing with classical greedy routing as the back up.

Fig. 9 illustrates the average delivery ratios of the five routing methods. Clearly, the delivery ratio increases when r_n increases. After r_n is larger than a certain value, it always guarantees the delivery. This also confirms our theoretical analysis of CTRs. In addition, we can conclude that the CTR for 3D greedy routing (approaching 100% delivery ratio when r_n is around 35 in Fig. 9) is just a little bit larger than the CTR for connectivity (network becomes connected when r_n is around 30 in Fig. 8). Notice that ERGrd methods without greedy backup have lower delivery ratio under the same circumstance, since they have smaller region to select the next hop node. With greedy backup, the delivery

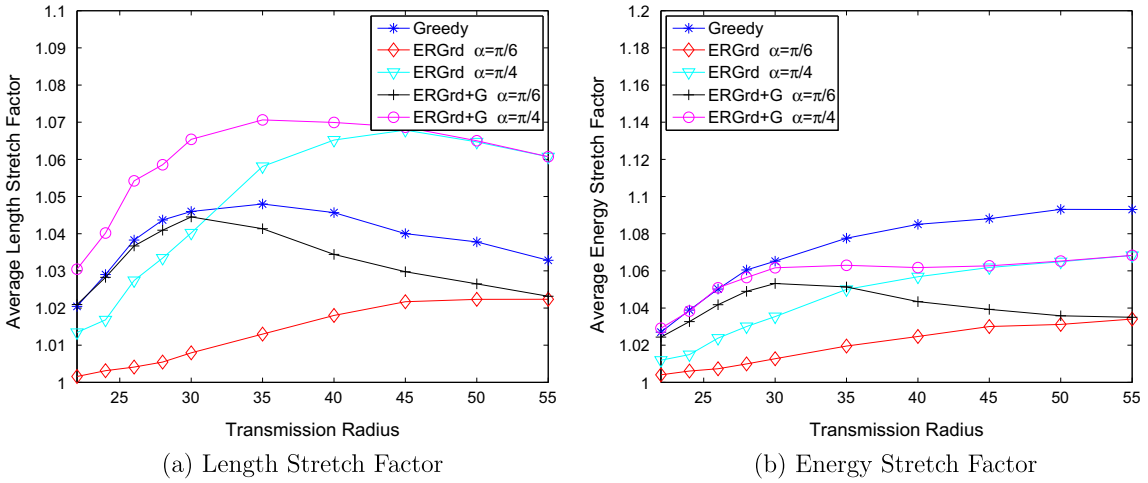

Fig. 10. Path efficiency (length stretch factor and energy stretch factor) of 3D greedy and 3D ERGrd routing methods in random networks.

ratios of ERGrd+Grd methods are almost the same with those of Grd (simple 3D greedy).

Fig. 10a and b illustrate the average length stretch factors and energy stretch factors of all routing methods, respectively. Here, the *length/energy stretch factor* of a path from node s to node t is the ratio between the total length/energy of this path and the total length/energy of the optimal path connecting s and t. Smaller stretch factor of a routing method shows better path efficiency. For the length stretch factor, the ERGrd with $\alpha = \pi/6$ has the best length efficiency. It is surprising that with $\alpha = \pi/4$ the length of ERGrd path could be longer than simple greedy. However, when considering the energy-efficiency, all ERGrd methods can achieve better path efficiency than simple greedy method. Notice that smaller restricted region leads to better path efficiency, however it also has lower delivery ratio. Therefore, it is a trade-off between path efficiency and packet delivery. It is also clear that when the network is dense (with large transmission radius), ERGrd and ERGrd+Grd are almost the same, since ERGrd can always find nodes inside the 3D cone. Notice that all the stretch factors in our simulations are near to 1.0, this is due to the uniform distribution of nodes. In practice, the stretch factors of simple greedy routing could be very large in the worst case.

Besides deploying random networks in a cubic region, we also performed simulations for networks deployed in a spherical region. The conclusions from these simulations are consistent with the simulations for random network deployed in cubic region.

7. Conclusion

In this paper, we study the design of 3D greedy routing for large-scale sensor networks. We first provide a theoretical analysis on the critical transmission radius for 3D greedy routing which leads to a delivery-guaranteed 3D localized routing. We theoretically prove that for a random 3D network, formed by nodes that are generated by a Poisson point process of density n over a convex compact region of unit volume, the critical transmission radius for 3D greedy routing is a.a.s. $\sqrt[3]{\frac{3\beta_0 \ln n}{4\pi n}}$, where $\beta_0 = 3.2$. This theoretical result answers a fundamental question about how large the transmission radius should be set in a 3D networks, such that the greedy routing guarantees the delivery of packets between any two nodes. We then refine the 3D greedy routing to a new localized routing protocol 3D ERGrd, which achieves the energy-efficiency by limiting its choice inside a restricted region and picking the node with best energy mileage. We also derive its critical transmission radius in random networks. Finally, we conduct extensive simulations to confirm our theoretical results. We believe that the proposed energy-efficient localized routing protocol is crucial for achieving sustainable and scalable in large-scale sensor networks.

Acknowledgment

The work of Y. Wang and M. Huang was supported in part by the US National Science Foundation under Grant No. CNS-0721666, CNS-0915331, and CNS-1050398. This work of C.-W. Yi was partially supported by NSC under Grant No. NSC97-2221-E-009-052-MY3 and NSC98-2218-E-009-023, and by the MoE ATU plan. His research is also supported by the Information and Communications Research Laboratories (ICL), Industrial Technology Research Institute (ITRI), Taiwan, Republic of China (ITRI Grant Project Code 9365C52200). The work of F. Li was partially supported by the National Natural Science Foundation of China (NSFC) under Grant 60903151.

References

[1] S. Durocher, D. Kirkpatrick, L. Narayanan. On routing with guaranteed delivery in three-dimensional ad hoc wireless networks, in: Proceedings of the 9th International Conference on Distributed Computing and Networking (ICDCN), 2008.
[2] R. Flury, R. Wattenhofer. Randomized 3D geographic routing, in: Proceedings of IEEE INFOCOM 2008, 2008.
[3] I.F. Akyildiz, D. Pompili, T. Melodia, Underwater acoustic sensor networks: research challenges, Ad Hoc Networks 3 (3) (2005) 257–279.
[4] X. Hong, M. Gerla, R. Bagrodia, T. Kwon, P. Estabrook, G. Pei. The Mars sensor network: efficient, energy aware communications. in: Proceedings of IEEE Military Communications Conference (MILCOM 2001), 2001.
[5] D. Pompili, T. Melodia. Three-dimensional routing in underwater acoustic sensor networks, in: Proceedings of ACM PE-WASUN 2005, Montreal, Canada, October 2005.
[6] P. Xie, J.-H. Cui, L. Lao. VBF: vector-based forwarding protocol for underwater sensor networks, in: Proceedings of IFIP Networking'06, 2006.
[7] P. Bose, P. Morin, I. Stojmenovic, J. Urrutia, Routing with guaranteed delivery in ad hoc wireless networks, ACM/Kluwer Wireless Networks 7 (6) (2001).
[8] B. Karp, H. Kung. GPSR: greedy perimeter stateless routing for wireless networks, in: Proceedings of the ACM International Conference on Mobile Computing and Networking, 2000.
[9] F. Kuhn, R. Wattenhofer, A. Zollinger. Worst-case optimal and average-case efficient geometric ad-hoc routing, in: Proceedings of the 4th ACM International Symposium on Mobile Ad-Hoc Networking and Computing (MobiHoc), 2003.
[10] T. Melodia, D. Pompili, I.F. Akyildiz. Optimal local topology knowledge for energy efficient geographical routing in sensor networks, in: Proceedings of IEEE INFOCOM, 2004.
[11] K. Seada, M. Zuniga, A. Helmy, B. Krishnamachari. Energy-efficient forwarding strategies for geographic routing in lossy wireless sensor networks, in: ACM Sensys, 2004.
[12] C-P. Li, W.-J. Hsu, B. Krishnamachari, A. Helmy. A local metric for geographic routing with power control in wireless networks, in: Proceedings of IEEE SECON, 2005.
[13] Y. Wang, W.-Z. Song, W. Wang, X.-Y. Li, T. Dahlberg. LEARN: localized energy aware restricted neighborhood routing for ad hoc networks, in: Proceedings of IEEE SECON, 2006.
[14] C.-F. Huang, Y.-C. Tseng, L.-C. Lo. The coverage problem in three-dimensional wireless sensor networks, in: Proceedings of IEEE Globecom 2004, 2004.
[15] S.M.N. Alam, Z.J. Haas. Coverage and connectivity in three-dimensional networks, in: Proceedings of the 12th ACM International Conference on Mobile Computing and Networking, 2006.
[16] M. Watfa, S. Commuri. Optimal 3-dimensional sensor deployment strategy, in: Proceedinga of the 3rd IEEE Consumer Communications and Networking Conference (CCNC), 2006.
[17] M. Watfa, S. Commuri. The 3-dimensional wireless sensor network coverage problem, in: Proceedings of IEEE International Conference on Networking, Sensing and Control (ICNSC), 2006.
[18] V. Ravelomanana, Extremal properties of three-dimensional sensor networks with applications, IEEE Transactions on Mobile Computing 3 (3) (2004) 246–257.
[19] Y. Wang, F. Li, T. Dahlberg. Power efficient 3-dimensional topology control for ad hoc and sensor networks, in: Proceedings of IEEE Global Telecommunications Conference (GlobeCom 2006), 2006.
[20] Y. Wang, L. Cao, T.A. Dahlberg, F. Li, X. Shi, Self-organizing fault tolerant topology control in large-scale three-dimensional wireless

networks, ACM Transactions on Autonomous and Adaptive Systems (TAAS) 4 (3) (2009) 19.1–19.21.
[21] G. Kao, T. Fevens, J. Opatrny. Position-based routing on 3-d geometric graphs in mobile ad hoc networks, in: Proceedings of CCCG 2005, 2005.
[22] A. Abdallah, T. Fevens, J. Opatrny. Power-aware 3d position-based routing algorithm for ad hoc networks, in: Proceedings of IEEE ICC 2007, 2007.
[23] F. Li, S. Chen, Y. Wang, J. Chen. Load balancing routing in three dimensional wireless networks, in: Proceedings of 2008 IEEE International Conference on Communications (ICC2008), 2008.
[24] C. Liu, J. Wu. Efficient geometric routing in three dimensional ad hoc networks, in: Proceedings of 27th Annual Joint Conference of IEEE Communication and Computer Society (INFOCOM) (Mini-conference), 2009.
[25] P. Gupta, P.R. Kumar. Critical power for asymptotic connectivity in wireless networks, in: W.H. Fleming, W.M. McEneaney, G. Yin, Q. Zhang (Eds.), Stochastic Analysis, Control, Optimization and Applications: A Volume in Honor, 1998.
[26] X.-Y. Li, P.-J. Wan, Y. Wang, C.-W. Yi, O. Frieder, Robust deployment and fault tolerant topology control for wireless ad hoc networks, Wiley Journal on Wireless Communications and Mobile Computing 4 (1) (2004) 109–125.
[27] M. Penrose, The longest edge of the random minimal spanning tree, Annals of Applied Probability 7 (1997) 340–361.
[28] C. Bettstetter. On the minimum node degree and connectivity of a wireless multihop network, in: Proceedings of 3rd ACM International Symposium on Mobile Ad Hoc Networking and Computing, 2002.
[29] P.-J. Wan, C.-W. Yi, F. Yao, X. Jia. Asymptotic critical transmission radius for greedy forward routing in wireless ad hoc networks, in: Proceedings of the 7th ACM International Symposium on Mobile Ad-Hoc Networking and Computing, 2006.
[30] L. Wang, C.-W. Yi, F. Yao. Improved asymptotic bounds on critical transmission radius for greedy forward routing in wireless ad hoc networks, in: Proceedings of the 9th ACM international Symposium on Mobile Ad Hoc Networking and Computing (MobiHoc '08), 2008.
[31] F. Baccelli, P. Bremaud, Elements of Queueing Theory: Palm–Martingale Calculus and Stochastic Recurrences, Springer, 2003.
[32] F.P. Preparata, M.I. Shamos, Computational Geometry: An Introduction, Springer-Verlag, 1985.
[33] P. Morin. Online routing in geometric graphs. PhD thesis, School of Computer Science, Carleton University, January 2001.
[34] X.-Y. Li, G. Calinescu, P.-J. Wan, Y. Wang, Localized Delaunay triangulation with applications in wireless ad hoc networks, IEEE Transactions on Parallel and Distributed Systems 14 (10) (2003) 1035–1047.
[35] J. Kuruvila, A. Nayak, I. Stojmenovic, Progress and location based localized power aware routing for ad hoc and sensor wireless networks, International Journal of Distributed Sensor Networks 2 (2006) 147–159.

Yu Wang is an Associate Professor of computer science at the University of North Carolina at Charlotte. He received his Ph.D. degree in Computer Science from Illinois Institute of Technology in 2004, his B.Eng. degree and M.Eng. degree in computer science from Tsinghua University, China, in 1998 and 2000. His research interest includes wireless networks, ad hoc and sensor networks, mobile computing, complex networks, and algorithm design. He has published more than 80 papers in peer-reviewed journals and conferences. He has served as program chair, publicity chair, and program committee member for several international conferences (such as IEEE INFOCOM, IEEE IPCCC, IEEE GLOBECOM, IEEE ICC, and IEEE MASS). He was the program co-chair of the first/second ACM International Workshop on Foundations of Wireless Ad Hoc and Sensor Networking and Computing (FOWANC 2008/2009), and was the program co-chair of the 26th IEEE International Performance Computing and Communications Conference (IEEE IPCCC 2007). He is a recipient of Ralph E. Powe Junior Faculty Enhancement Awards from Oak Ridge Associated Universities in 2006 and a recipient of Outstanding Faculty Research Award from College of Computing and Informatics at UNC charlotte in 2008. He is a member of the ACM and a senior member of the IEEE, and IEEE Communications Society.

Chih-Wei Yi received his PhD degree from the Illinois Institute of Technology in 2005, and BS and MS degrees from the National Taiwan University in 1991 and 1993, respectively. He is currently an Associate Professor in Computer Science at the National Chiao Tung University. He is a member of the IEEE and the ACM. He had been a Senior Research Fellow of the Department of Computer Science, City University of Hong Kong. He was awarded the Outstanding Young Engineer Award by the Chinese Institute of Engineers in 2009. His research focuses on wireless ad hoc and sensor networks, vehicular ad hoc networks, network coding, and algorithm design and analysis.

Minsu Huang received his BS degree in computer science from Central South University in 2003 and his MS degree in computer science from Tsinghua University in 2006. He is currently a PhD student in the University of North Carolina at Charlotte, majoring in computer science. His current research focuses on wireless networks, ad hoc and sensor networks, and algorithm design.

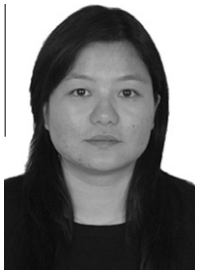

Fan Li received the PhD degree in computer science from the University of North Carolina at Charlotte in 2008, M.Eng. degree in electrical engineering from the University of Delaware in 2004, the M.Eng. degree and B.Eng. degree in communications and information system from Huazhong University of Science and Technology, China. She is currently an associate Professor of school of computer science at Beijing institute of Technology. Her current research focuses on wireless networks, ad hoc and sensor networks, and mobile computing.